

References and Notes

1. M. Kimura, *The Neutral Theory of Molecular Evolution* (Cambridge Univ. Press, Cambridge, 1983).
2. M. Nei, *Molecular Evolutionary Genetics* (Columbia Univ. Press, New York, 1987).
3. W.-H. Li, *Molecular Evolution* (Sinauer, Sunderland, MA, 1997).
4. N. J. Tourasse, W.-H. Li, *Mol. Biol. Evol.* **17**, 656 (2000).
5. D. Mazel, P. Marlière, *Nature* **341**, 245 (1989).
6. N. M. Kredich, in *Escherichia coli and Salmonella typhimurium*, F. C. Neidhardt, Ed. (American Society for Microbiology, Washington, DC, 1996), pp. 419–429.
7. D. Thomas, Y. Surdin-Kerjan, *Microbiol. Mol. Biol. Rev.* **61**, 503 (1997).
8. H. Cherest, D. Thomas, Y. Surdin-Kerjan, *J. Bacteriol.* **175**, 5366 (1993).
9. T. S. Leyh, Y. Suo, *J. Biol. Chem.* **267**, 542 (1992).
10. T. S. Leyh, *Crit. Rev. Biochem. Mol. Biol.* **28**, 515 (1993).
11. For *S. cerevisiae*, the sulfur-assimilatory enzymes used for the statistical analyses were the *MET1*, 2, 3, 4, 5, 6, 7, 8, 10, 13, 14, 16, 25, 28, 31, 32, *STR1*, *STR4*, *SUL1*, and *SUL2* gene products. For *E. coli*, the en-

- zymes used were the *CysA*, *B*, *C*, *D*, *E*, *G*, *H*, *I*, *J*, *K*, *M*, *N*, *P*, *U*, *W*, *Z*, *MetA*, *B*, *C*, *E*, *H*, *R*, and *Sbp* gene products.
12. S. Karlin, V. Brendel, *Science* **257**, 39 (1992).
13. S. Karlin, B. E. Blaisdell, P. Bucher, *Protein Eng.* **5**, 729 (1992).
14. For all the calculations reported here, the methionine initiating residues were removed from all the protein sequences.
15. T. E. Creighton, *Proteins: Structures and Molecular Properties* (Freeman, New York, 1983).
16. N. Suekhoa, *Cold Spring Harbor Symp. Quant. Biol.* **26**, 35 (1961).
17. G. A. C. Singer, D. A. Hickey, *Mol. Biol. Evol.* **17**, 1581 (2000).
18. P. Baudouin-Cornu, Y. Surdin-Kerjan, P. Marlière, D. Thomas, data not shown.
19. O. W. Griffith, *Methods Enzymol.* **143**, 366 (1987).
20. Supplementary material is available on Science Online at www.sciencemag.org/cgi/content/full/293/5528/297/DC1.
21. W. D. Kruger, D. R. Cox, *Proc. Natl. Acad. Sci. U.S.A.* **91**, 6614 (1994).
22. D. G. Fraenkel, in *Escherichia coli and Salmonella typhimurium*, F. C. Neidhardt, Ed. (American Society for Microbiology, Washington, DC, 1996), pp. 189–198.

23. M. Johnston, M. Carlson, in *The Molecular and Cellular Biology of the Yeast Saccharomyces*, E. W. Jones, J. R. Pringle, J. R. Broach, Eds. (Cold Spring Harbor Laboratory Press, Cold Spring Harbor, NY, 1992), pp. 193–281.
24. For *S. cerevisiae*, the carbon-assimilatory enzymes used for the statistical analyses were the *ENO1*, *ENO2*, *FBA1*, *FBP1*, *GLK1*, *GMP1*, *HXX1*, *HXX2*, *PDC1*, *PDC5*, *PDC6*, *PFK1*, *PFK2*, *PGI1*, *PGK1*, *PYC1*, *PYK1*, *TDH1*, *TDH2*, *TDH3*, *TPI1*, and *ZWF1* gene products. For *E. coli*, the enzymes used were the *Eno*, *FbaA*, *GapA*, *Glk*, *Gnd*, *GpmA*, *PfkA*, *PfkB*, *Pgi*, *Pgk*, *Pgm*, *PykA*, *RpE*, *RpiA*, *RpiB*, *TalB*, *TktA*, *TktB*, *TpiA*, and *Zwf* gene products.
25. B. Magasanik, in *The Molecular and Cellular Biology of the Yeast Saccharomyces*, E. W. Jones, J. R. Pringle, J. R. Broach, Eds. (Cold Spring Harbor Laboratory Press, Cold Spring Harbor, NY, 1992), pp. 283–317.
26. The *S. cerevisiae* nitrogen-assimilatory enzymes used for the statistical analyses were the *DAL1*, 2, 3, 4, 5, 7, 81, *DUR3*, *DUR12*, *GDH1*, *GDH2*, *PUT1*, 2, 3, 4, *UGA1*, 3, 4, and 5 gene products.
27. Supported by a thesis fellowship from the Ministère de la Défense (P.B.-C.).

26 March 2001; accepted 1 June 2001

Impairment of Mycobacterial But Not Viral Immunity by a Germline Human *STAT1* Mutation

Stéphanie Dupuis,^{1,2} Catherine Dargemont,³ Claire Fieschi,¹ Nicolas Thomassin,⁴ Sergio Rosenzweig,⁵ Jeff Harris,⁶ Steven M. Holland,⁵ Robert D. Schreiber,⁷ Jean-Laurent Casanova^{1,8*}

Interferons (IFN) α/β and γ induce the formation of two transcriptional activators: gamma-activating factor (GAF) and interferon-stimulated gamma factor 3 (ISGF3). We report a natural heterozygous germline *STAT1* mutation associated with susceptibility to mycobacterial but not viral disease. This mutation causes a loss of GAF and ISGF3 activation but is dominant for one cellular phenotype and recessive for the other. It impairs the nuclear accumulation of GAF but not of ISGF3 in heterozygous cells stimulated by IFNs. Thus, the antimycobacterial, but not the antiviral, effects of human IFNs are principally mediated by GAF.

Mendelian susceptibility to mycobacterial disease is a rare syndrome (MIM 209950), leading to severe clinical infections with weakly virulent mycobacterial species, such as *Bacillus Calmette-Guérin* (BCG) vaccines (1) or environmental nontuberculous mycobacteria (2) and more virulent *Mycobacterium tuberculosis* (3). Other types of microorganisms rarely cause severe clinical disease, except for *Salmonella*, which infects less than half of the patients. Null recessive mutations have been identified in *IL12B* (4), encoding the p40 subunit of interleukin-12 (IL-12), in *IL12RB1* (5, 6), encoding the $\beta 1$ chain of the IL-12 receptor, in *IFNGR1* (7, 8), and in *IFNGR2* (9), encoding the two chains of the IFN- γ receptor (IFN- γ R). Recessive and dominant mutations, associated with partial

IFN- γ R, deficiency, have been found in *IFNGR1* (3, 10) and *IFNGR2* (11). These studies established that human IL-12-dependent IFN- γ -mediated immunity is essential to control mycobacteria and provided means of molecular diagnosis and rational treatment based on pathophysiology. However, no clear genetic etiology has been identified for a number of patients.

We investigated two unrelated patients with unexplained mycobacterial disease. Proband 1 (P1) is a 33-year-old French woman who developed disseminated BCG infection in childhood (12). She had experienced many common viral infections, the clinical course of which was normal. Mutations in *IL12B* and *IL12RB1* had been excluded (13). We characterized cellular responses to IFN- γ by

electrophoretic mobility shift assay (EMSA) using Epstein-Barr virus (EBV)-transformed B (EBV-B) cells. The level of nuclear-protein binding to gamma interferon-activating sequences (GAS) in P1 cells stimulated with IFN- γ (Fig. 1A) was $25 \pm 3\%$ of that in identically treated control cells (14). The GAS-binding protein, designated gamma-activating factor (GAF), consisted of STAT-1/STAT-1 homodimers (13). This profile was similar to that observed in partial IFN- γ R1 and IFN- γ R2 deficiency, but mutations in *IFNGR1* and *IFNGR2* were excluded (13). Moreover, only $25 \pm 2\%$ of the GAF detected in control cells was detected in P1 cells stimulated with IFN- α (13). Thus, the binding of nuclear STAT-1 homodimers to GAS was affected equally by IFN- γ and IFN- α in P1 cells.

We then analyzed the subcellular distribution of STAT-1 in simian virus 40 (SV40)-transformed fibroblasts (SV40 fibroblasts) by immunofluorescence (15). A smaller proportion of P1 STAT-1 accumulated in the nucleus upon IFN- γ stimulation than in control cells (Fig. 1B). This suggested that the smaller number of GAS-binding STAT-1 dimers

¹Laboratoire de Génétique Humaine des Maladies Infectieuses, Université de Paris René Descartes-INSERM UMR550, Faculté de Médecine Necker-Enfants Malades, 75015 Paris, France. ²INSERM U429, Hôpital Necker-Enfants Malades, 75015 Paris, France. ³Institut Jacques Monod, CNRS-Université Paris VI-Université Paris VII-CNRS UMR7592, 75005 Paris, France. ⁴Département de Pédiatrie, Centre Hospitalier Général, 58000 Nevers, France. ⁵Laboratory of Host Defenses, National Institute of Allergy and Infectious Diseases, Bethesda, MD 20892-1886, USA. ⁶Department of Pediatrics, University of California at San Francisco, San Francisco, CA 94117, USA. ⁷Department of Pathology, Washington University, St. Louis, MO 63110, USA. ⁸Unité d'Hématologie-Immunologie Pédiatrique, Hôpital Necker-Enfants Malades, 75015 Paris, France.

*To whom correspondence should be addressed. E-mail: casanova@necker.fr

REPORTS

was due to low levels of nuclear GAF and not to a low affinity of nuclear STAT-1 for GAS. Tyrosine 701 phosphorylation is essential for STAT-1 dissociation from IFN- γ R1, homodimerization, and nuclear translocation (16). We therefore subjected EBV-B cells to immunoprecipitation with a STAT-1-specific mAb and immunoblotting with a STAT-1-phosphotyrosine 701-specific Ab (17). After stimulation with IFN- α or IFN- γ , the level of tyrosine 701 phosphorylation was lower in P1 than in control cells (Fig. 1C). Similar results were obtained by immunoblotting with a phosphotyrosine-specific monoclonal antibody (13). In contrast, similar levels of serine 727-phosphorylated STAT-1 were detected in P1 and control cells (18). This suggests that in P1 cells, STAT-1 molecules are poorly phosphorylated at tyrosine 701 in response to both IFN- α and IFN- γ . This probably accounts for the impaired nuclear accumulation and DNA binding of GAF.

We investigated the DNA binding activity of STAT-1/STAT-2/p48 trimers, known as interferon-stimulated gamma factor 3 (ISGF3) (14). Similar levels of IFN-stimulated response element (ISRE)-binding complex were detected in control and P1 EBV-B cells after IFN- α stimulation (Fig. 1D). Supershift experiments confirmed that the ISRE-binding complex consisted of ISGF3 (13). The subcellular distribution of ISGF3 was then analyzed in SV40 fibroblasts with a STAT-2-specific mAb (15). IFN- α stimulation resulted in strong nuclear accumulation of STAT-2 molecules in both control and P1 cells (Fig. 1E). ISGF3 activation in response to IFN- γ (19) was not detected in our exper-

imental conditions. Thus, GAF activation was impaired in P1 cells stimulated by IFN- α and - γ , whereas ISGF3 activation by IFN- α was not affected. We investigated IFN- α - and IFN- γ -inducible gene transcription by Northern blotting (20). *P48* transcription was induced by IFN- γ in control but not P1 cells, whereas *MXA* transcription was induced by IFN- α in both control and P1 cells (Fig. 1F). The dissociation of IFN-induced signaling pathways mediated by GAF and ISGF3 is therefore functionally relevant for IFN-responsive target genes.

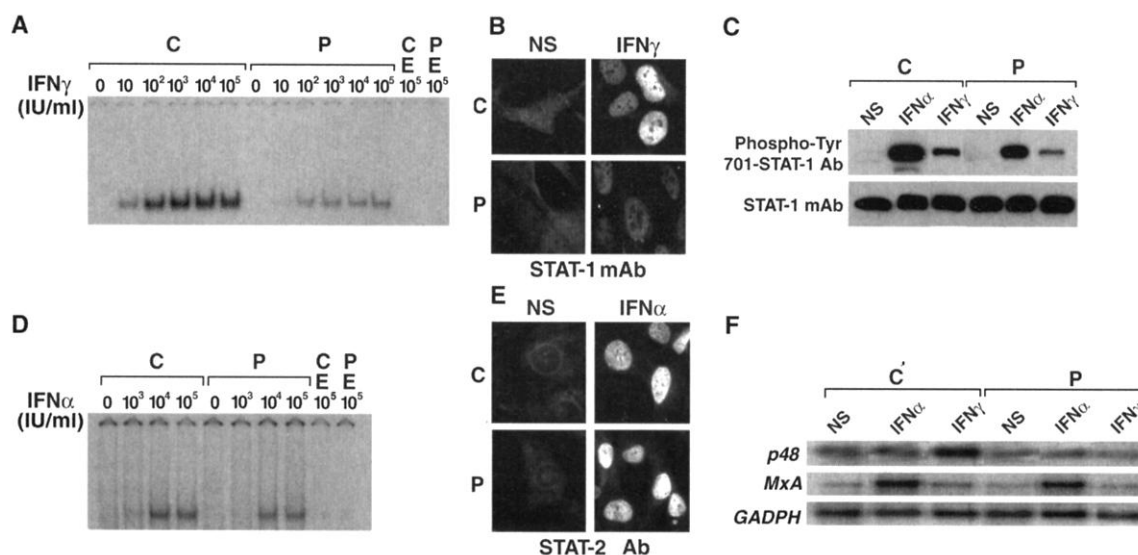
We searched for mutations in the two molecules known to be shared by the IFN- α/β and IFN- γ signaling pathways, JAK-1 and STAT-1. Sequencing of the P1 *JAK1* coding region revealed no mutation (13). Sequencing of the *STAT1* gene and cDNA revealed a heterozygous substitution (T \rightarrow C) at nucleotide position 2116 of the coding region, resulting in a serine (S) for leucine (L) substitution at amino acid position 706 (L706S) (21) (Fig. 2A). The L706S mutation was not found in the patient's parents (Fig. 2B), suggesting that the mutational event occurred in one of the parental germ-lines. P1 transmitted the mutation to her daughter. Unlike all other family members, P1 and her daughter displayed the same abnormal cellular phenotype, with impaired activation of GAF, but not ISGF3, in response to both IFN- γ and IFN- α (13). The L706S mutation was not found in 50 unrelated healthy individuals examined. *STAT1* was also sequenced in 50 patients with mycobacterial disease. An unrelated patient (proband 2, P2) was found to be heterozygous for the L706S mutation (Fig. 2B). P2 is a 10-year-old American girl who developed

Mycobacterium avium infection at 6 years of age (22). These findings strongly suggest a causal relationship between heterozygosity for the *STAT1* L706S allele and vulnerability to mycobacteria.

We transiently transfected a mouse fibroblast cell line deficient in STAT-1 with wild-type or L706S human *STAT1* alleles or an insert-less vector (23). No STAT-1 was detected in cells transfected with insert-less vector (13). In IFN- γ -stimulated cells, wild-type STAT-1 accumulated in the nucleus, whereas L706S STAT-1 remained cytoplasmic (Fig. 3A). Similarly, stimulation by IFN- α led to the nuclear accumulation of both STAT-1 and STAT-2 in cells transfected with the wild-type *STAT1* allele, but not in cells transfected with the L706S allele (Fig. 3B). This demonstrates a loss of function for the L706S *STAT1* allele, in the nuclear accumulation of GAF and ISGF3 in response to both IFN- γ and IFN- α . Staining with a STAT-1-phosphotyrosine 701-specific antibody demonstrated the phosphorylation of nuclear wild-type STAT-1, but not of cytoplasmic L706S STAT-1 upon IFN- γ stimulation (Fig. 3C). This is consistent with previous experiments in heterozygous cells (Fig. 1C) and strongly suggests that L706S is a loss-of-function mutation, principally because it severely impairs the phosphorylation of tyrosine 701.

Transient transfections were carried out with various ratios of wild-type and L706S *STAT1* alleles. The nuclear accumulation of STAT-1 upon IFN- γ stimulation was impaired with a 7:3 ratio and completely inhibited with a 3:7 ratio (13), indicating that the

Fig. 1. Cellular responses to IFN- γ and IFN- α . (A) GAS probe-binding nuclear proteins from EBV-B cells from a control (C) and the patient (P), in response to various concentrations of IFN- γ , as determined by EMSA. An excess of unlabeled probe is indicated by "E." (B) Subcellular distribution of STAT-1 in SV40 fibroblasts from a control (C) and the patient (P), either not stimulated (NS) or stimulated with IFN- γ (10^5 IU/ml), as shown by indirect immunofluorescence. (C) Tyrosine 701 phosphorylation of STAT-1 in EBV-B cells from a control (C) and the patient (P), either not stimulated (NS) or stimulated with IFN- α or IFN- γ (10^5 IU/ml), as determined by STAT-1 immunoprecipitation followed by immunoblotting of tyrosine 701-phosphorylated STAT-1 or total STAT-1 molecules. (D) ISRE probe-binding nuclear proteins from EBV-B cells from a control (C) and the patient (P), in response to various concentrations of IFN- α , as determined by EMSA. (E)



(F) Levels of *p48*, *MXA*, and *GADPH* mRNAs in EBV-B cells from a control (C) and the patient (P), either not stimulated (NS) or stimulated with IFN- α (10^4 IU/ml) or IFN- γ (10^2 IU/ml), as detected by Northern blotting.

REPORTS

L706S *STAT1* null allele exerts a dominant-negative effect over the wild-type allele for GAF activation. Three of the four possible STAT-1 combinations recruited to the IFN receptor in wild-type/L706S cells are probably nonfunctional because at least one component cannot be phosphorylated on tyrosine

701. One functional combination (wild type/wild type) is responsible for the 25% residual activity. L706S STAT-1 binding to IFN- γ R1 has not been assessed. Although the L706S *STAT1* allele also causes a loss of function for ISGF3 activation, it is recessive for this phenotype. Crystallographic studies established

the crucial role of leucine 706 for STAT-1 homodimerization (24), and STAT-2 has been shown to be recruited first by the IFN- α receptor (25). Thus, L706S STAT-1 is unlikely to dimerize with IFN- α -bound phosphorylated STAT-2, and sufficient wild-type STAT-1 is probably available in heterozygous cells to form functional ISGF3 complexes. The dimerization of L706S STAT-1 with STAT-2 has not been assessed.

The clinical phenotype of these patients is similar to that of patients with partial IFN- γ R deficiency (3, 10, 11). Thus, human IFN-mediated antimycobacterial immunity involves principally STAT-1-dependent, GAF-dependent, IFN- γ -stimulated pathways. IFN- γ R knockout mice are vulnerable to mycobacteria (26), but the status of IFN- α R (27, 28) and STAT-1 (29, 30) knockout mice is not known. Heterozygous L706S *STAT1* mutation does not compromise antiviral immunity, as the three STAT-1-deficient individuals reported here were resistant to all viruses they had been exposed to. IFN- α R (27, 28, 31), STAT-1 (29, 30, 31), and STAT-2 (32) knockout mice are susceptible to all viruses tested, suggesting that mouse IFN- α -mediated antiviral immunity is in part ISGF3-dependent. STAT-1-independent effects of IFN- α also contribute to immunity against viruses in mice (31). Thus, either small amounts of GAF are sufficient to protect the patients against viruses, or, more probably, GAF plays no major role in IFN- α -mediated antiviral immunity in humans. IFN- α -stimulated ISGF3 activation, which is preserved in patients carrying the L706S *STAT1* mutation, or STAT-1-independent IFN- α -stimulated pathways, presumably intact as well, are probably essential for human antiviral immunity.

Fig. 2. *STAT1* genotype and cellular and clinical phenotype. (A) STAT-1, with its coiled-coil (CC), DNA-binding (DNA-B), Src-homology 2 (SH2), tail segment (TS), and transactivation (TA) domains and the positions of tyrosine 701 (Y701), leucine 706 (affected by mutation L706S), and serine 727 (S727). (B) *STAT1* genotype and cellular and clinical phenotype in the two kindreds. Healthy individuals with two wild-type copies of *STAT1* are shown in white. L706S heterozygous P1 (A.II.2) with BCG infection is shown in black, and her heterozygous daughter, with a cellular but currently no clinical phenotype, is indicated by a vertical bar. Heterozygous P2 (B.II.1) with *M. avium* infection is shown in black.

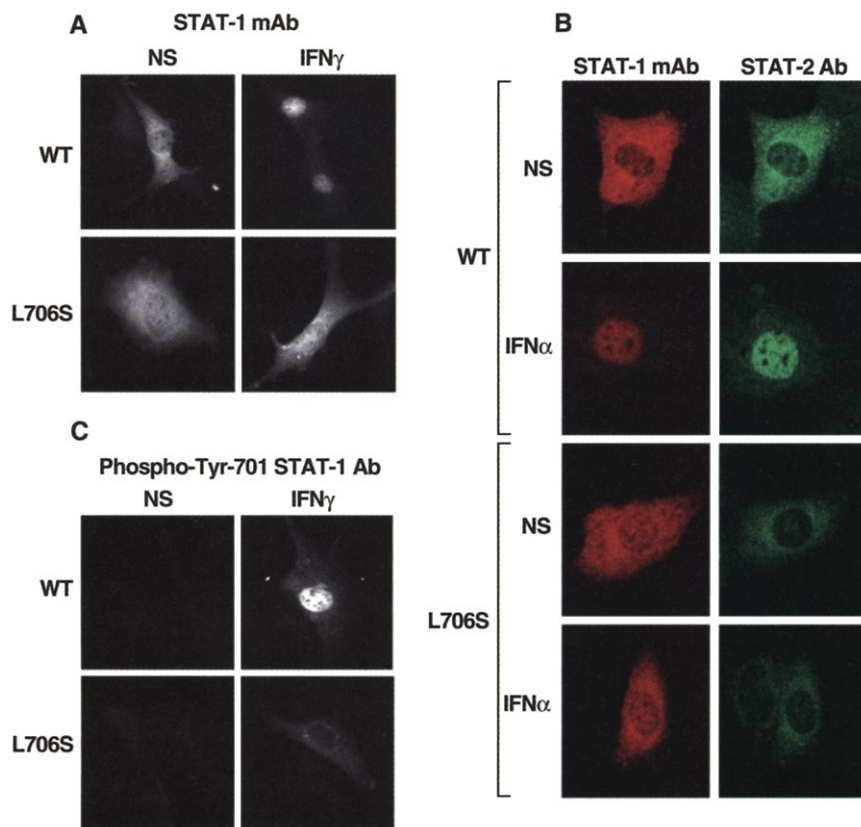
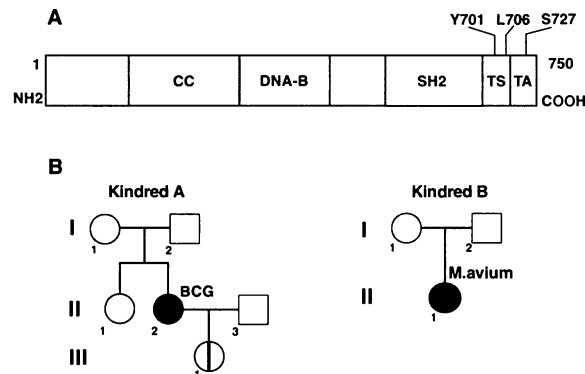


Fig. 3. Characterization of the mutant *STAT1* allele. (A) Subcellular distribution of human STAT-1 in mouse STAT-1-deficient fibroblasts, either not stimulated (NS) or stimulated with murine IFN- γ (10^5 IU/ml), after transfection with wild-type (WT) or mutant (L706S) human *STAT1* allele, as detected by indirect immunofluorescence. (B) Subcellular localization of human STAT-1 and mouse STAT-2 in mouse STAT-1-deficient fibroblasts, either not stimulated (NS) or stimulated with murine IFN- α (10^5 IU/ml), after transfection with the wild-type (WT) or mutant (L706S) human *STAT1* allele, as detected by indirect immunofluorescence with a confocal microscope. (C) Tyrosine 701 phosphorylation of human STAT-1 in mouse STAT-1-deficient fibroblasts, either not stimulated (NS) or stimulated with IFN- γ (10^5 IU/ml), after transfection with the wild-type (WT) or mutant (L706S) human *STAT1* allele, as detected by indirect immunofluorescence.

References and Notes

1. J.-L. Casanova *et al.*, *Pediatrics* **98**, 774 (1996).
2. M. Levin *et al.*, *Lancet* **342**, 79 (1993).
3. E. Jouanguy *et al.*, *J. Clin. Invest.* **100**, 2658 (1997).
4. F. Altare *et al.*, *J. Clin. Invest.* **102**, 2035 (1998).
5. F. Altare *et al.*, *Science* **280**, 1432 (1998).
6. R. de Jong *et al.*, *Science* **280**, 1435 (1998).
7. M. J. Newport *et al.*, *N. Engl. J. Med.* **335**, 1941 (1996).
8. E. Jouanguy *et al.*, *N. Engl. J. Med.* **335**, 1956 (1996).
9. S. E. Dorman, S. M. Holland, *J. Clin. Invest.* **101**, 2364 (1998).
10. E. Jouanguy *et al.*, *Nature Genet.* **21**, 370 (1999).
11. R. Dörfinger *et al.*, *J. Infect. Dis.* **181**, 379 (2000).
12. F. Verliac *et al.*, *Infections Osseuses Bactériennes non Tuberculeuses* (Expansion Scientifique, Paris, 1972). No recurrence of BCG infection occurred until the patient's last followup at 33 years of age. She had self-healing clinical illnesses caused by human herpesvirus 6, parvovirus B19, papillomavirus, herpes simplex, varicella-zoster, Epstein-Barr, measles, mumps, rubella, respiratory syncytial, and influenza viruses, as attested by specific serum immunoglobulin G (IgG) levels. Her daughter, now 3 years of age, was not inoculated with BCG. She also had benign human herpes virus 6, parvovirus B19, and herpes simplex virus infections.
13. S. Dupuis *et al.*, data not shown.
14. Nuclear extracts from EBV-B cells, unstimulated or stimulated with human IFN- γ (Boehringer) or IFN- α 2b (Schering-Plough) for 30 min, were subjected to EMSA (3) with either a GAS (5'-ATGTATTCCCA-

gAAA-3') or an ISRE radiolabeled probe (5'-gATCggg-AAAAGgAAACCgAAACTgAA-3'). The signal was quantified with a phosphorimager (Amersham).

15. SV40 fibroblasts, unstimulated or stimulated with IFN- γ or IFN- α for 30 min, were fixed with 3% paraformaldehyde or 100% methanol at -20°C and permeabilized with 0.1% Triton X-100 (Sigma). The fibroblasts were incubated with mouse monoclonal antibody to STAT-1 (N-Terminus; Transduction Laboratories) or rabbit antibody to STAT-2 (sc476; Santa Cruz) for 30 min, followed by fluorescein isothiocyanate (FITC)-conjugated antibody to mouse or antibody to rabbit for 30 min (Jackson).
16. C. V. Ramana, M. Chatterjee-Kishore, H. Nguyen, G. R. Stark, *Oncogene* **19**, 2619 (2000).
17. Lysates from EBV-B cells, either not stimulated or stimulated with IFN- α or IFN- γ for 30 min, were immunoprecipitated with a monoclonal antibody to STAT-1 IgG1 (Sc417; Santa Cruz). Immune complexes were analyzed by 8% SDS-polyacrylamide gel electrophoresis (SDS-PAGE) and Western blotting. The polyvinylidene fluoride membrane was probed with a rabbit antibody to phosphotyrosine 701-STAT-1 (9171L; New England Biolabs) or a mouse antibody to STAT-1 (Sc417; Santa Cruz). Bound antibodies were detected by enhanced chemiluminescence (Amersham).
18. See the supplementary material, available on Science Online at www.sciencemag.org/cgi/content/full/293/5528/300/DC1.
19. A. Takaoka et al., *Science* **288**, 2357 (2000).
20. EBV-B cells were stimulated with IFN- α or IFN- γ for 2 hours, and total RNA was analyzed by Northern blotting (4). The nylon membrane was probed with P48-, MxA-, or GDAPH-specific radiolabeled DNA fragments (available upon request).
21. The STAT1 cDNA was amplified with sense (5'-TCgACAgTCTTggCACCTAACgTgC-3') and antisense (5'-TgCTATCAACaggTgCAGcG-3') primers. The STAT1 exon encoding L706 was amplified with sense (5'-TCggTgATggAAAgCgTA-3') and antisense (5'-CTCTCTgTgTCACTTAC-3') primers. Genomic DNA from various tissues (blood, hair roots, and buccal cells) and cell lines (EBV-B cells and SV40 fibroblasts) was amplified. The products were sequenced as previously described (10).
22. The patient was not vaccinated with BCG and had benign illnesses caused by cytomegalovirus and varicella-zoster virus, as attested by serum-specific IgG antibodies.
23. Two days after electroporation with pcDNA3-WT-STAT-1 (provided by M. J. Holtzman), pcDNA3-L706S-STAT-1, or a mock vector, mouse STAT-1-deficient embryonic fibroblasts were stimulated with murine IFN- γ (R&D) or IFN- α (Gibco BRL) for 30 min. Indirect immunofluorescence, with a mouse monoclonal antibody to human STAT-1 (N-Terminus; Transduction Laboratories) or a rabbit antibody specific to STAT-1-phosphotyrosine 701 (9171L; New England Biolabs) was performed as in (18). Double immunofluorescence was performed by incubation with a mouse antibody to human STAT-1 (N-Terminus; Transduction Laboratories) and a rabbit antibody to mouse STAT-2 Ab (provided by C. Schindler) for 30 min, followed by a tetramethyl rhodamine isothiocyanate-conjugated mouse antibody (Jackson) and FITC-conjugated rabbit antibody (Jackson) for 30 min as described by C. Park et al. [*Nucleic Acids Res.* **27**, 4191 (1999)]. The cells were visualized by confocal microscopy (Zeiss).
24. X. Chen et al., *Cell* **93**, 827 (1998).
25. S. A. Qureshi, S. Leung, I. M. Kerr, G. R. Stark, J. E. Darnell Jr., *Mol. Cell. Biol.* **16**, 288 (1996).
26. R. Kamijo et al., *J. Exp. Med.* **178**, 1435 (1993).
27. U. Muller et al., *Science* **264**, 1918 (1994).
28. M. F. van den Broek, U. Muller, S. Huang, R. M. Zinkernagel, M. Aguet, *Immunol. Rev.* **148**, 5 (1995).
29. J. E. Durbin, R. Hackenmiller, M. C. Simon, D. E. Levy, *Cell* **84**, 443 (1996).
30. M. A. Meraz et al., *Cell* **84**, 431 (1996).
31. M. P. Gil et al., *Proc. Natl. Acad. Sci. U.S.A.*, **98**, 6680 (2001).
32. C. Park, S. Li, E. Cha, C. Schindler, *Immunity* **13**, 795 (2000).
33. We thank L. Abel, S. Pellegrini, J. Puck, and J. C. Weill for

helpful discussions and M. J. Holtzman, D. Frank, D. Recan, and C. Schindler for providing cells or reagents. J.-L.C. would like to thank A. Munnich for support and encouragement. This work was supported by grants from Action Incitative Concertée Blanche, Banque Nationale de Paris-Paribas, Fondation pour la Recherche

Médicale, Fondation Schlumberger, Legs Poix, Programme National de Recherche Fondamentale en Microbiologie, Maladies Infectieuses et Parasitaires, and Institut Universitaire de France.

29 March 2001; accepted 7 June 2001

Interferon- γ -Mediated Site-Specific Clearance of Alphavirus from CNS Neurons

Gwendolyn K. Binder and Diane E. Griffin*

Recovery from viral encephalomyelitis requires immune-mediated noncytolytic clearance from neurons by mechanisms assumed to be the same for all neurons. In alphavirus encephalomyelitis, antibody clears infectious virus from neurons in all regions of the central nervous system (CNS), but CD8 T cells contribute to elimination of viral RNA. To understand the role of T cells in clearance, we infected antibody knockout mice with Sindbis virus. Virus was cleared from spinal cord and brain stem neurons, but not from cortical neurons, and required both CD4 and CD8 T cells. Infection with cytokine-expressing recombinant viruses suggested that T cells used interferon- γ , but not tumor necrosis factor α , in clearing virus and that populations of neurons differ in responsiveness to this effector pathway.

Viral infections of brain and spinal cord neurons necessitate development of an immune response within the central nervous system (CNS). However, local infiltration of inflammatory cells provides the potential for immune-mediated neurologic damage. Because recovery from viral encephalitis can occur without permanent neurologic damage, noncytolytic mechanisms of clearance must exist. To investigate these mechanisms, we studied a model of murine encephalomyelitis induced by infection with Sindbis virus (SV), a mosquito-borne alphavirus related to western and eastern equine encephalitis viruses. SV infects neurons in both the brain and spinal cord (1) and induces a well-characterized immune response in the CNS (2-4) that results in clearance of infectious virus within 7 to 8 days without paralysis or death. Thus, SV encephalomyelitis provides an excellent model for identifying the immune mechanisms responsible for effective noncytolytic clearance of virus from the CNS.

Previous studies that used passive transfer of antibody into severe combined immune deficiency (SCID) mice persistently infected with SV showed that antibody is a primary mediator of noncytolytic clearance of infectious virus from neurons in both the brain and spinal cord (3). However, antibody-indepen-

dent cytolytic and noncytolytic T cell-mediated control of virus replication occurs in nonneural tissues (5-7). Such mechanisms have been considered irrelevant to virus clearance from neurons, in part because of the restricted expression of major histocompatibility class I and class II antigens by these cells (8). Consistent with this view, clearance of infectious SV from neurons is normal in mice deficient in CD8 T cells. However, clearance of viral RNA is slowed in these mice, suggesting an auxiliary role for T cells (9).

To investigate whether alternate mechanisms of noncytolytic viral clearance exist, we infected C57BL/6 antibody knockout (μ MT) mice (10) with the TE strain of SV (11) and examined clearance of infectious virus from the brain and spinal cord. As controls, immunocompetent wild-type C57BL/6 and immunodeficient SCID mice (Fig. 1, A and B) were infected with the same SV strain (12). Initial levels of virus replication were similar in all mice, and, although wild-type mice cleared infectious virus from the brain and spinal cord between days 6 and 9 after infection, SCID mice established persistent infection in the brain and spinal cord but developed no neurological symptoms. During the first 2 weeks of infection, virus titers in brains of μ MT mice were intermediate between those of SCID and wild-type mice, but later, titers were similar to those of SCID mice. In contrast, infectious virus was completely cleared from the spinal cords of μ MT mice with a time course that was only slightly slower than that of wild-type mice.

W. Harry Feinstone Department of Molecular Microbiology and Immunology, Johns Hopkins University Bloomberg School of Public Health, Baltimore, MD 21205, USA.

*To whom correspondence should be addressed. E-mail: dgriffin@jhsp.edu